Can. J. Remote Sensing, Vol. 29, No. 5, pp. 633–649, 2003

Combined high-density lidar and multispectral imagery for individual tree crown analysis

Don Leckie, François Gougeon, David Hill, Rick Quinn, Lynne Armstrong, and Roger Shreenan

Abstract. Lidar technology has reached a point where ground and forest canopy elevation models can be produced at high spatial resolution. Individual tree crown isolation and classification methods are developing rapidly for multispectral imagery. Analysis of multispectral imagery, however, does not readily provide tree height information and lidar data alone cannot provide species and health attributes. The combination of lidar and multispectral data at the individual tree level may provide a very useful forest inventory tool. A valley following approach to individual tree isolation was applied to both high resolution digital frame camera imagery and a canopy height model (CHM) created from high-density lidar data over a test site of even aged (55 years old) Douglas-fir plots of varying densities (300, 500, and 725 stems/ha) on the west coast of Canada. Tree height was determined from the laser data within the automated crown delineations. Automated tree isolations of the multispectral imagery achieved 80%–90% good correspondence with the ground reference tree delineations based on ground data. However, for the more open plot there were serious commission errors (false trees isolated) mostly related to sunlit ground vegetation. These were successfully reduced by applying a height filter to the isolations based on the lidar data. Isolations from the lidar data produced good isolations with few commission errors but poorer crown outline delineations especially for the densest plot. There is a complimentarity in the two data sources that will help in tree isolation. Heights of the automated isolations were consistently underestimated versus ground reference trees with an average error of 1.3 m. Further work is needed to test and develop tools and capabilities, but there is an effective synergy of the two high resolution data sources for providing needed forest inventory information.

Résumé. La technologie lidar a atteint un stade où les modèles d'élévation du sol et du couvert forestier peuvent être produits à des résolutions spatiales élevées. Les méthodes de délimitation et de classification des couronnes au niveau de l'arbre individuel se développent rapidement dans le domaine des images multispectrales. L'analyse des images multispectrales cependant ne fournit pas directement d'information sur la hauteur des arbres et les données lidar par elles-mêmes ne peuvent fournir les attributs d'espèce et de santé. La combinaison des données lidar et multispectrales au niveau de l'arbre individuel pourrait constituer un outil très utile d'inventaire forestier. Une approche basée sur la détection et le suivi des vallées d'ombres pour réaliser la délimitation des arbres individuels a été appliquée à des images haute résolution acquises par caméra numérique et à un modèle de hauteur du couvert créé à partir de données lidar haute densité au-dessus d'un site d'étude composé de parcelles de pins Douglas d'âge égal (55 ans) et de densité variable (300, 500 et 725 tiges/ha), sur la côte ouest du Canada. La hauteur des arbres a été déterminée à l'aide des données laser dans le cadre d'un processus de délimitation automatique des couronnes. La délimitation automatique des arbres réalisée à l'aide des images multispectrales a donné une bonne correspondance de l'ordre de 80 % à 90 % comparativement aux résultats de la délimitation des arbres au sol basée sur les données de terrain. Toutefois, dans le cas de la parcelle plus ouverte, on observe des erreurs importantes de commission (faux arbres isolés) reliées principalement à l'illumination de la végétation au sol par le soleil. Celles-ci ont été réduites avec succès suite à l'application d'un filtre de hauteur aux délimitations basées sur les données lidar. Les délimitations réalisées à l'aide des données lidar ont produit de bons résultats avec peu d'erreurs de commission mais avec des délimitations de profils de couronne plus faibles, particulièrement dans le cas de la parcelle la plus dense. Il existe une complémentarité dans les deux sources de données qui aide à la délimitation des arbres. Les hauteurs des délimitations automatiques étaient sous-estimées de façon constante par rapport aux arbres de référence au sol, avec une erreur moyenne de 1,3 m. Des travaux additionnels sont nécessaires pour tester et développer des outils et améliorer le potentiel de ces données, mais il existe néanmoins une synergie efficace entre ces deux sources de données haute résolution dans l'apport d'information essentielle pour les inventaires forestiers.
[Traduit par la Rédaction]

Introduction

Background

Forest stand attribute information such as species composition, crown closure, height, and age along with derived volumes form the basis of forest management planning in many jurisdictions worldwide. These are usually acquired on a descriptive basis from aerial photographic interpretation. Forest

Received 24 July 2002. Accepted 12 May 2003.

D. Leckie,[1] F. Gougeon, and D. Hill. Pacific Forestry Centre, Canadian Forest Service, Natural Resources Canada, 506 West Burnside Road, Victoria, BC V8Z 1M5, Canada.

R. Quinn, L. Armstrong, and R. Shreenan. Terra Remote Sensing Inc., 1962 Mills Road, Sidney, BC V8L 5Y3, Canada.

[1]Corresponding author (e-mail: dleckie@pfc.forestry.ca).

operations planning is based on more detailed information derived from individual tree data gathered from ground plots. This includes number of trees and their species, diameter breast height (DBH), height, age, and wood quality parameters. Environmental and wildlife considerations are also important along with the presence of snags, canopy gaps, diversity, and other factors. In addition there is a wide variety of information required for specific needs, such as decisions on thinning, post-harvest surveys after partial cutting, insect and disease damage assessment, and regeneration monitoring. Each of these special purpose surveys has its own needs and is done with a variety of combinations of methods based on ground, remote sensing, and aerial observation. Therefore, a wide suite of stand and individual tree information is required.

A remote sensing survey system that could capture information on a single tree basis would provide much of the needed information and improve forest inventory at a stand level, reduce the number of field plots needed, and fulfill the needs of a variety of special purpose surveys. The combination of optical imagery, whether it is digitized aerial photography or multispectral sensors, with airborne laser data may provide a powerful suite of data for extracting the needed information (Leckie, 1990). High resolution imagery in which individual trees can be separated and assessed is needed. This is available in airborne multispectral sensors and panchromatic imagery from satellite systems such as IKONOS (Space Imaging, Thornton, Colo.) and QuickBird (DigitalGlobe, Longmont, Colo.), which are at the 1 m and 61 cm levels, respectively. It is also now possible to have airborne laser data acquired with contiguous small footprints so that high resolution height images can be created. Discrete pulse systems with pulse rates of 10–50 kHz are operational. New laser technology developments are also permitting data to be acquired from higher altitudes (Baltsavias, 1999), so that it is possible to simultaneously acquire lidar data and optical imagery at altitudes normally flown for the aerial photography used for forest inventory (i.e., scales of 1:10 000 to 1:20 000). In addition, with both multispectral imagery and airborne laser data, the sensors, processing methods, data storage, and computing power needed are at or approaching a stage where not only site specific projects are feasible, but large area surveys such as those over management units are also possible.

Methods for automated analysis of high resolution (<1 m) digital imagery on an individual tree basis are progressing and have shown operational capabilities (Hill and Leckie, 1999). The approach is to locate and (or) delineate individual tree crowns, determine species, and extract information such as stem density and distribution, crown closure, crown size, canopy gaps, and health condition. A variety of methods for identifying and delineating individual trees are available and have shown promising results. These methods are based on finding local maxima in the image, matching physical models of trees to the imagery in template matching techniques, methods such as the valley following approach that utilize the "topography" in the image intensity formed by the bright reflectance from trees and darker intensities on the crowns or gaps between them due to shading, or combinations of these and other techniques (e.g., Gougeon and Moore, 1989; Pinz, 1991; Gougeon, 1995a; Pollock, 1996; Larsen, 1997; Dralle and Rudemo, 1997; Uuttera et al., 1998; Warner et al., 1999; Wulder et al., 2000; Quackenbush et al., 2000; Tarp-Johansen, 2001; Culvenor, 2002; Pouliot et al., 2002). Effectiveness varies depending on the tree and stand conditions, data source, resolution and algorithm used. Individual tree species and tree damage have been classified, mostly by methods based on the spectral content of the automatically identified trees (Gougeon, 1995b; Leckie and Gougeon, 1999; Key et al., 2001; Haara and Nevalainen, 2002). Success has varied with good results in simple stand conditions and problems in complex stands.

The focus of developments regarding the use of lidar data in forestry has been on terrain mapping and estimating stand height. There have been several main approaches to extracting stand height depending on the laser data and sensor. Early laser profiling systems acquired often closely spaced small footprint data on a single transect or profile. Scanning lidars collect sample laser points on a spaced pattern. These earlier systems could record only the first return, thus indicating the elevation of the tree or ground surface. Current systems can often record the first and last returns or the intensity of returns in between. Two important issues regarding tree or stand height estimation with such systems are (*i*) determining the elevation of the ground by properly separating the laser returns from the ground, and (*ii*) the laser hits from the tree canopy do not all represent the top of the tree, but various positions along the canopy surface envelope. Nevertheless, some success has been achieved with such approaches using various simple and complex techniques (Schrieirer et al., 1985; Nilsson, 1996; Næsset, 1997; Magnussen and Boudewyn, 1998; Næsset and Bjerknes, 2001; Tickle et al., 2001; Popescu et al., 2002). These methods are directed at estimating stand height and usually use a fraction of the highest returns within a sample area to represent the heights of the higher trees in a stand (e.g., window-based quantile estimators). Another approach is to use wide footprint lidar such that the footprint will usually include several tree crowns and thus the first return will be a response from near the apex of the highest tree in the crown and the last return is often from the ground surface. These systems use first and last returns or record multiple returns through the canopy (Aldred and Bonnor, 1985; MacLean and Krabill, 1986; Harding et al., 2001). The Vegetation Canopy Lidar (Dubayah et al., 1997) is a proposed satellite lidar system designed on these principles to estimate vegetation height. Multiple return and continuous wave systems have also been used to estimate various other stand parameters such as biomass, basal area, and vertical distribution of foliage (Nelson et al., 1988; Lefsky et al., 1999; Means et al., 1999). One issue is that the first return from these systems being a wide footprint can often be offset below the crown apex of the highest tree owing to lack of a sufficient triggering signal. Height information on shorter trees within the footprint cannot be definitively extracted. Also, the ground surface elevation and microrelief can vary within the footprint in some terrains and this affects height estimates. In

all systems and methods, it can be a problem to ensure that there are enough laser pulses penetrating the canopy and returning from the ground. In addition, there can be difficulties determining whether a given laser return is from the ground and not from a distance above it because of dense ground or understory vegetation.

Recent sensor developments make high-density spacing small-footprint lidar data possible, in essence creating laser height "imagery" at resolutions of 70 cm and less. This gives a representation of the three-dimensional shape of individual tree crowns. If individual tree locations can be extracted from the data, or other data such as optical high resolution imagery, the troublesome issues present with noncontiguous scanned laser data can be solved. There would be a laser hit covering the top of each tree and one would know which hits they are. The issues with the broad footprint approach of not getting a signal from the highest tree, not capturing height information for other shorter trees, and errors caused by microrelief are also potentially resolved. Some work has been conducted on this type of data (Andersen et al., 2001; Hyyppä et al., 2001a; Næsset and Økland, 2002, Persson et al., 2002), but exploration of the possibilities and methods is just beginning.

It is as yet unclear how well trees can be isolated independently with high resolution lidar, but it is expected that a combination of information from the multispectral imagery and lidar and their crown isolations would be useful. Once trees are well isolated regardless of the process, tree height would be extracted from the lidar data within that tree. This may be the highest sample point under the tree or the highest point of the digital canopy model. Most information on individual tree species and health is expected to come from the multispectral data, but three-dimensional crown shape, texture or outline, and vertical distribution of laser returns within a crown may also be helpful. Both spectral- and lidar-based tree delineations can lead to crown size and closure estimates. Analysis of each or both data sources combined, independent of any tree crown delineation (e.g., use of a simple height threshold on the lidar data), can also provide closure information. The best method, data source, or use of synergy between data sources or methods needs to be examined.

It is envisioned that a future system will be able to routinely provide simultaneous multispectral imagery and high resolution laser "imagery" to extract individual tree crowns and information on their species, crown area, stand closure, and vertical structure. Indeed laser return intensity or reflectance images at vertical slices through the canopy will be produced. Using laser systems at different wavelengths, multispectral vertical slices may be possible. It may even be possible to extract fluorescence data, which have been related to vegetation vigour or health (Chappelle and Lichtenthaler, 1994; Lüdeker et al., 1999; Saito et al., 2000). The value of the laser intensity images, and certainly slices through the canopy is unknown; explorations need to begin.

Objective

The main objective of this paper is to explore possible benefits of combining multispectral and lidar data at an individual tree level for providing forest inventory information. A particular focus is their possible combined use for automated tree isolation and the capabilities of using lidar data for determining heights of trees as represented by the automated isolations. This paper presents the above concepts, assembles a data set of combined high resolution multispectral and lidar data, examines the use of existing preprocessing tools and a valley following tree isolation method on both lidar and multispectral data sets, explores the synergy between the two types of data, and presents a simple application of tree isolation using multispectral imagery combined with lidar data followed by height extraction on an individual tree basis.

The effectiveness of the two different data sources for isolating trees for low and moderate density conifer plots is documented. The sources of error for each is examined. From this information the synergy and usefulness of combining data sources for tree isolation is discussed. The use of elevation data to eliminate false alarms on the multispectral data and the use of a minimum size criterion for both data sets is demonstrated. Once trees are isolated, height estimation accuracy is determined. The height estimates for the following cases are examined: (*i*) manually outlined ground reference trees to determine the accuracy of height estimates if there is no error or bias caused by the automated isolation process, (*ii*) automated isolations that matched ground reference trees well, and (*iii*) if all isolations (including omissions and commissions) are considered giving the combined effect of isolation and height error on stand height estimation. Sources of error in the height estimation are discussed. Also compared are heights determined from the highest laser hit within the isolation boundaries versus the highest point in the canopy height model (CHM).

Sites

The data used in this study are part of a larger data set acquired over a site on Vancouver Island, approximately 30 km northwest of Victoria, British Columbia. The site includes existing plots and silviculture trial experiments within the Greater Victoria Watershed District and sites in an area adjacent and north of the watershed consisting of the Shawnigan Lake Fertilizer Trials (Crown and Brett, 1975) and Canadian Forest Service LOGS (levels of growing stock) site (Beddows, 2002). Six sites were overflown in total: three chronosequence plots (Trofymow et. al., 1998), which contain varying age classes and densities of Douglas-fir and other species; Rithet Creek, a site with mature Douglas-fir adjacent to a young Douglas-fir plantation (Wulder et al., 2000); plus the fertilizer and LOGS trials. Each site contains plots with full stem maps and records of species, DBH, a sample of tree heights, and records of understory and ground vegetation cover.

This study uses data from the LOGS site, which is a test of growth rates and wood characteristics for Douglas-fir grown under different thinning regimes. It consists of even aged Douglas-fir (55 years old) with eight thinning treatments ranging from 259 stems/ha to untreated control plots at 2100 stems/ha (**Figure 1**). There are twenty-seven 28.5 m × 28.5 m (0.081 ha) treatment plots each with a 20 m × 20 m measurement plot centered within it. Three plots were used for this study (**Figure 1**, **Table 1**), representing low to moderate conifer stem densities. They are plot 19 (heavy thinning), plot 20 (moderate thinning), and plot 18 (medium-heavy to light thinning). Crown length was typically between 6 and 11 m.

The understory in all plots contained various densities of salal (*Gaultheria shallon* Pursh), with lesser amounts of bracken (*Pteridium aquilinum pubescens* (L.) Kuhn) along with Oregon grape (*Mahonia nervosa* Nutt.), red huckleberry (*Vaccinium parvifolium* Sm.), and moss (mainly *Eurynchium*

Table 1. Characteristics of LOGS plots.

Stand parameter	Plot 19	Plot 20	Plot 18
Density (stems/ha)	300	500	725
Avg. height (m)	26.2	25.2	24.4
Height (SD) (m)	2.00	1.94	2.42
Avg. DBH (cm)	36.2	30.2	30.7
DBH (SD) (cm)	2.50	7.87	5.28
Avg. crown diameter (m)	7.0	5.8	5.6
Crown diameter (SD) (m)	1.12	0.96	0.76

Note: DBH, diameter breast height; SD, standard deviation.

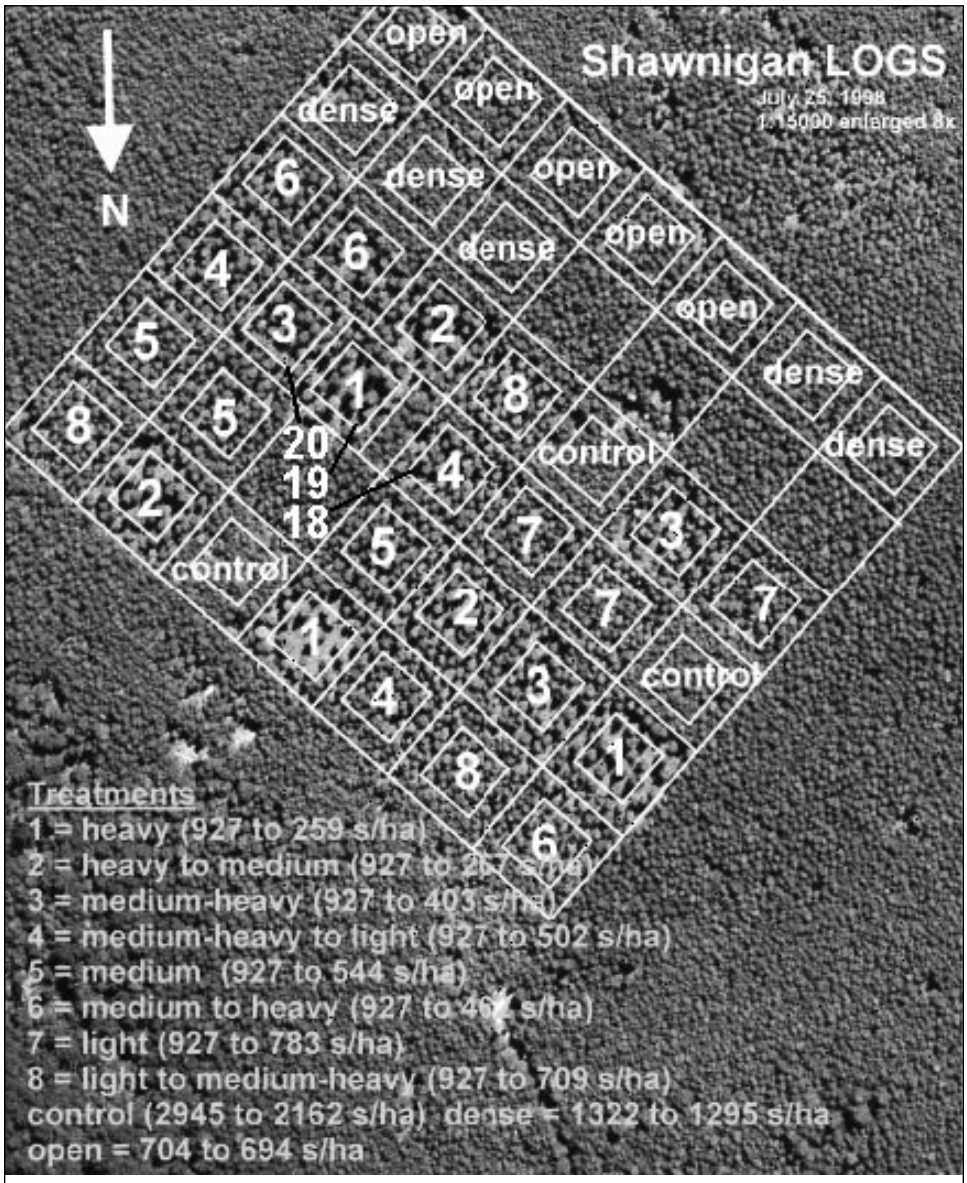

Figure 1. The different thinning treatments within the Shawnigan LOGS site containing plots 18, 19, and 20 used in this study (adapted from Beddows, 2002). For the treatments, 927 stems/ha was the starting or baseline density before the treatments and the second number is the target stems/ha after the latest thinning.

oreganum (Sull.) Jacq.). For plots 18, 19, and 20, the salal was quite dense (75%–90% of ground vegetation) and ranged from 0.5 to 1.1 m in height. There were also patches of bracken, typically 1–2 m high, overtopping the salal. Ground vegetation covered 100% of the plots.

Digital frame camera imagery and lidar data

Data acquisition

Digital frame camera (DFC) and lidar data were acquired simultaneously from a helicopter by Terra Remote Sensing Inc. (Sidney, B.C.). For the LOGS site there were four flight lines, two side lapping lines at azimuth 310° along the long axis direction of the plots, and two adjacent perpendicular lines. Flying altitude was 265 m above ground level and ground speed was 14.5 m/s. Flights were on 19 August 2001 at 10:40 PDT giving a sun elevation and azimuth of 37° and 117°, respectively. The positioning system consisted of a Litton LTN-92 inertial navigation system (INS) and an Astech Z-surveyor Dual Frequency P-code Differential Geographic Positioning System (DGPS). The INS provides accurate attitude parameters (roll, pitch, and yaw). The DGPS supplies absolute position coordinates for rectifying and geocoding image data. The DGPS receivers record the aircraft's altitude and position to accuracies of 5 to 10 cm. The imagery itself is time-stamped to a millisecond precision during acquisition with a (DGPS) slaved time annotator.

Sensors were in a pod beneath the helicopter. The multispectral imagery was acquired with a Kodak digital camera with a 2008 × 3040 pixel array, Nikon 28-mm lens, and field of view of 51° × 35°. This provides three bands of data, one each in the red, green, and blue parts of the spectrum. The resolution of the imagery was 8.5 cm. Width of a frame was 250 m along track and 170 m across. Frame rate gave a 30% overlap. The adjacent flight lines provided 60% side lap. For the individual frames used for the three field plots analyzed in this study (plots 18, 19, and 20), plot centers were at 22°, 7°, and 6° off nadir, respectively. Forward/Nadir Video Camera data were also recorded to provide a broader view and reference.

Lidar data were acquired with Terra Remote Sensing's Terrain Scanning Lidar, a proprietary Lightwave Model 110 scanning lidar system with a pulse repetition frequency of 10 kHz. It is a diode-pumped YAG laser with a wavelength of 1047 nm, a swath width of 56°, and a beam divergence of 3.5 mrad. It scans in a continuous mode in a zigzag pattern and for this project had an accuracy of 27 cm horizontal and 15 cm vertical. Footprint size was approximately 93 cm. Each flight line had laser hit spacing of 0.5 m across track and 1.0 m along track. Average spot density was therefore 2/m^2. First-return hits only were recorded.

To achieve higher spot densities to test high-density lidar data, the lidar data from all four flight lines were combined (after geometric correction). Data from two flight lines contributed to plot 18, and data from four flight lines contributed to plots 19 and 20. This generated average spacings of 25 cm between footprints and average spot densities of 8/m^2 for plots 18, 19, and 20, with spacings varying from 10 to 40 cm (**Figure 2**).

Preprocessing of lidar data

The lidar data were geometrically corrected by Terra Remote Sensing using the DGPS-derived aircraft locations and INS data. Processing of the lidar points results in positioning of points to within 30 cm *xy* and ±15 cm in *z*. Each flight line was processed separately and then combined in Terrascan software to produce point coverages. The software was used to separate ground and canopy hits and to create separate point coverages for each. This process produced ground points interpolated and gridded to a 1-m point grid.

The ground grid was then processed to produce a digital elevation model of the LOGS site. PCI EASI/PACE software was used to generate a digital elevation model (DEM) using the program VDEMINT. This was done to a 25-cm pixel resolution to match the average spacing of the lidar hits. This provides the ground surface from which tree heights are measured. A merging of all hits, ground and canopy, was generated and this was used in subsequent analysis of the canopy envelope, tree height, and tree isolation. Spacings are variable and sometimes patterned, but are high. Generalized three-dimensional tree shapes are visible but there are variations from a smooth surface. One notable issue is the occurrence of low values "holes", or indeed ground hits within a tree crown. These can be caused by penetration through the canopy. However, they are also caused by merging the data sets from different flight lines. If a tree, especially those in open stands, is viewed from the side, it is possible to receive an uninterrupted laser hit from the ground under the vertical projection of the crown. When properly placed in *xy* position, this appears as a ground hit within the canopy.

To minimize the effect of these canopy "holes", a CHM was developed in a manner that eliminated many of the holes. This was done by assigning lidar hits from all flight lines to 25-cm grid cells. A filtering was then conducted on the data in which only the highest lidar return in each cell was retained. The data were then used to generate the surface model. This eliminated many of the ground hits from within canopies but some remained and caused artifacts in the surface model.

A CHM was then developed giving a surface representation of the canopy envelope. The VDEMINT routine, within PCI software, was used to generate the CHM. The VDEMINT procedure is based on a distance transform algorithm that interpolates between vector points and uses a finite difference method to iteratively smooth the resulting raster surface. The finite difference method does not change the original elevation points, but does update the interpolated values based on neighbourhood values. While computationally efficient, this procedure is designed to produce DEMs of the ground surface and does not have special provision to account for spiked

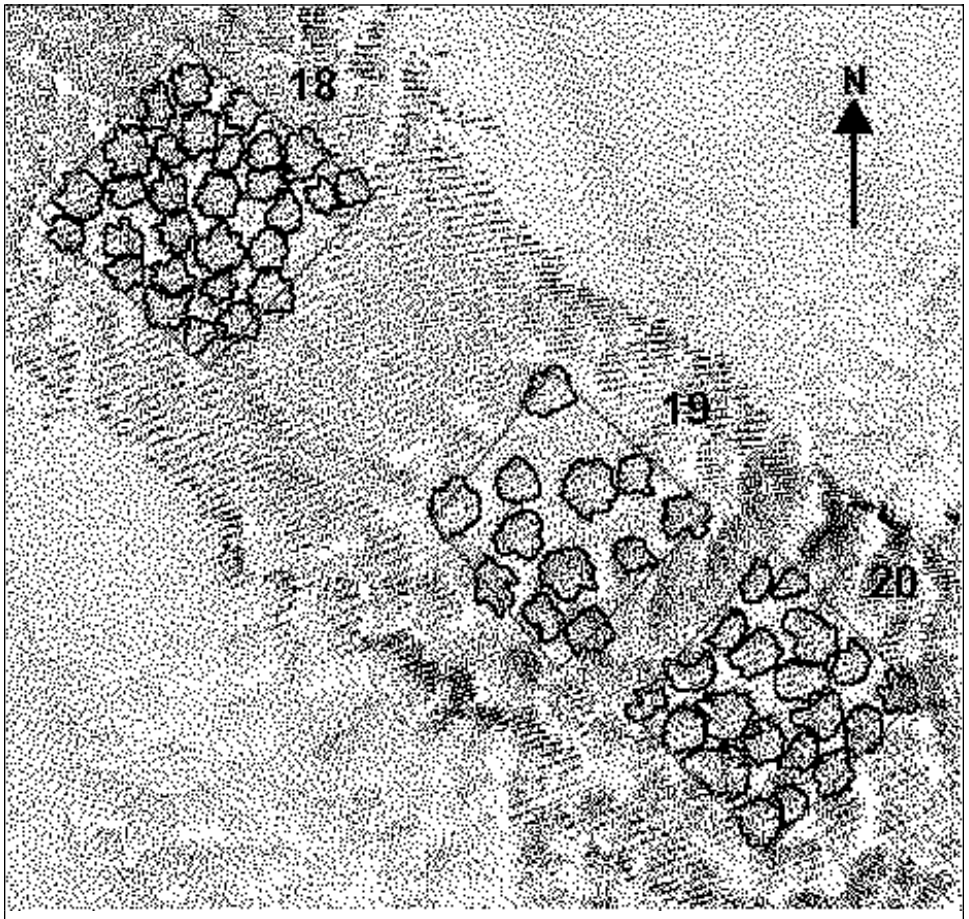

Figure 2. Lidar returns from the four flight lines over LOGS site plots 18, 19, and 20.

surfaces, which lidar points within trees may represent, and has no knowledge or provision to account for the expected shapes of trees. **Figure 3** gives the resulting surface model with 25-cm postings for the area around plots 18, 19, and 20. Representation of the tree crown shapes is reasonable in general. There appears to be shape texture within the crowns (depressions or a facetted structure), but this may be related to the processing techniques or slightly anomalous heights.

Preprocessing of DFC imagery

The digital camera frames were individually orthorectified. Rectification was again done with standard existing software (PCI Orthoengine). Resampling was to 25 cm via a cubic convolution resampling kernel. The CHM generated from the lidar data was used as the surface model for the orthorectification. Both manual delineation of tree crowns and automated crown isolation were conducted on these individual orthorectified frames. The manual delineations and isolation boundaries on each frame were then overlain on the CHM.

Individual tree isolation

The valley following approach of Gougeon (1995a) was used for delineating trees on both the DFC and lidar data. The method is part of a software package (Individual Tree Crown suite; Gougeon, 2000). The method and its variants have shown good results in conifer stands, especially moderately dense stands (Andrew et al., 1999; Leckie et al., 1999a). It is based on the assumption that on spectral imagery, trees are represented by bright pixels surrounded by lower intensity pixels in shaded areas or less illuminated parts of the crown. In essence, it is treating the intensity image like a topographic surface, thus it is a well-suited algorithm for isolating trees on lidar data as well. It finds local minima and follows valleys from these into the canopy and between trees. This valley following procedure creates a binary mask of areas considered valleys (valley material) and potential tree crown material. A second rule-based routine follows the edges of each island of crown material in a clockwise fashion and determines if it is a shape appropriate for a tree. There is provision for splitting crown material into two units if there is an indentation in the shape that can be jumped to join with valley material on the opposite side. The outlines produced by the process are meant to represent isolations of tree crowns and are referred to as "isols".

Isolations were done using the orthorectified individual digital camera image frames resampled to 50-cm resolution. The green spectral band was used as the intensity image, and a smoothing via a 3 × 3 average filter was applied before

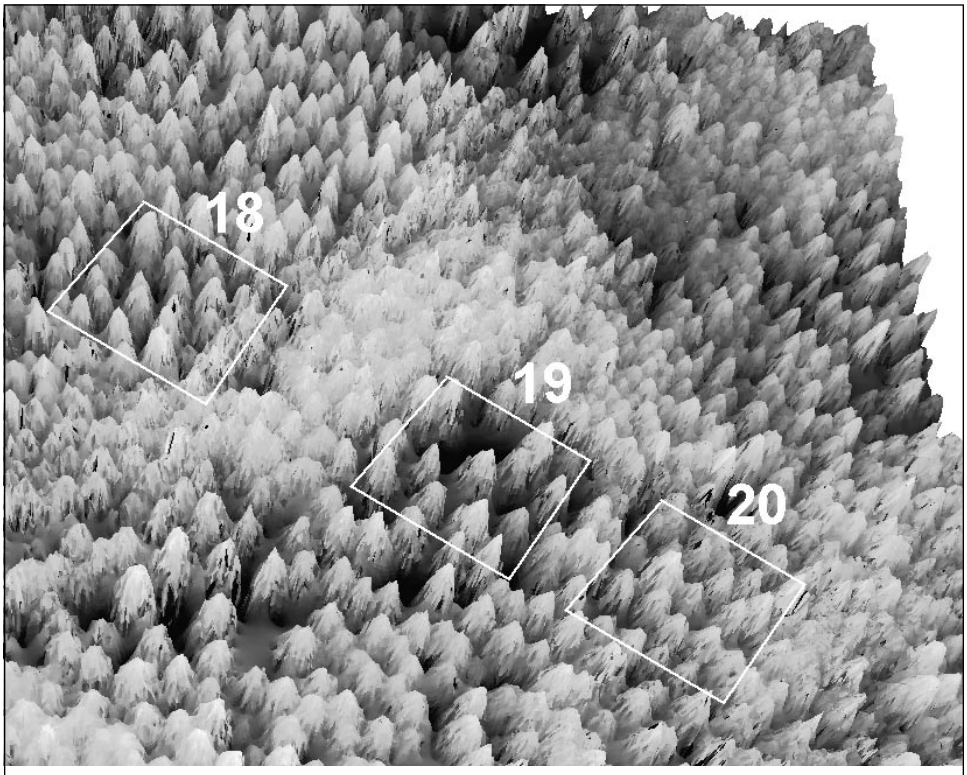

Figure 3. Canopy height model (25-cm grid) generated from the lidar hits.

isolation. **Figure 4** gives an example of the resulting isols. Similarly for the lidar data, the 25-cm CHM was resampled to 50 cm and a 3 × 3 average filtering conducted before isolation (**Figure 5**).

As a secondary process applied to both the multispectral and lidar isolations, small isols of <7 m^2, well below the minimum size of tree expected for the plots, were screened out. This limit was chosen to be very conservative and to err on the side of including commission errors rather than omitting actual trees. It represents the mean crown diameter minus three standard deviations (3 m). In an additional process, the lidar data were used to eliminate isolations with no height. Isols with a maximum lidar height within them of <2 m were filtered out. Two meters represents the approximate maximum height of the ground vegetation on the plots. This prevented anomalous isols, related to spectral features on the ground resembling trees, from being considered tree crowns.

Verification data and methods

While in the field, crown locations and outlines for each tree in the plots were mapped onto prints of the DFC imagery. Care was taken to outline crowns accounting for shadowed portions of the crown or large individual branches extending from the main crown. Where trees were touching or for suppressed trees (there were few in the plots), the boundary of the intersection of the crowns was outlined. Prints of the lidar data were also used in the field to add information to help outline the trees. For each tree in the plots, species, height (to top of leader and to last whorl), diameter at breast height, crown diameter in two directions, and height to live crown were measured. Field work was conducted in late May 2002, before any growth had occurred. Stem maps and previous field measurements were also available for each plot.

The tree outlines as marked in the field were transferred on-screen onto the DFC imagery as vectors (**Figure 4a**). These outlines referred to as ground reference delineations (greds) were then used as a truth boundary for comparison with the automatically generated tree delineations. Since the DFC imagery is orthorectified to the lidar generated CHM, the greds were also registered to the lidar data. An ITC software routine MARA (manual to automated recognition accuracy) was used to compare delineations. Twenty types of overlap relevant to delineation accuracy assessment are defined (Leckie et al., 1999b). A "perfect" match with a ground reference delineation is declared when there is a one-to-one correspondence (i.e., only one isol associated with one gred and only one gred associated with that isol) and their respective overlaps are greater than 50%. Other cases of "good" matches are a one-to-one correspondence, but the isol is too big and cases where there may be several isols associated with a gred but overlap of the secondary isol on the gred is minor and only a small portion of the secondary isol is located within the gred. Cases where there are several isols within a gred are considered poor and are termed a split ground reference delineation. Isols with several greds falling largely within them are termed grouped. Isols not associated with a gred are commission errors. Correspondence of the automated isolations with the tree crowns as represented

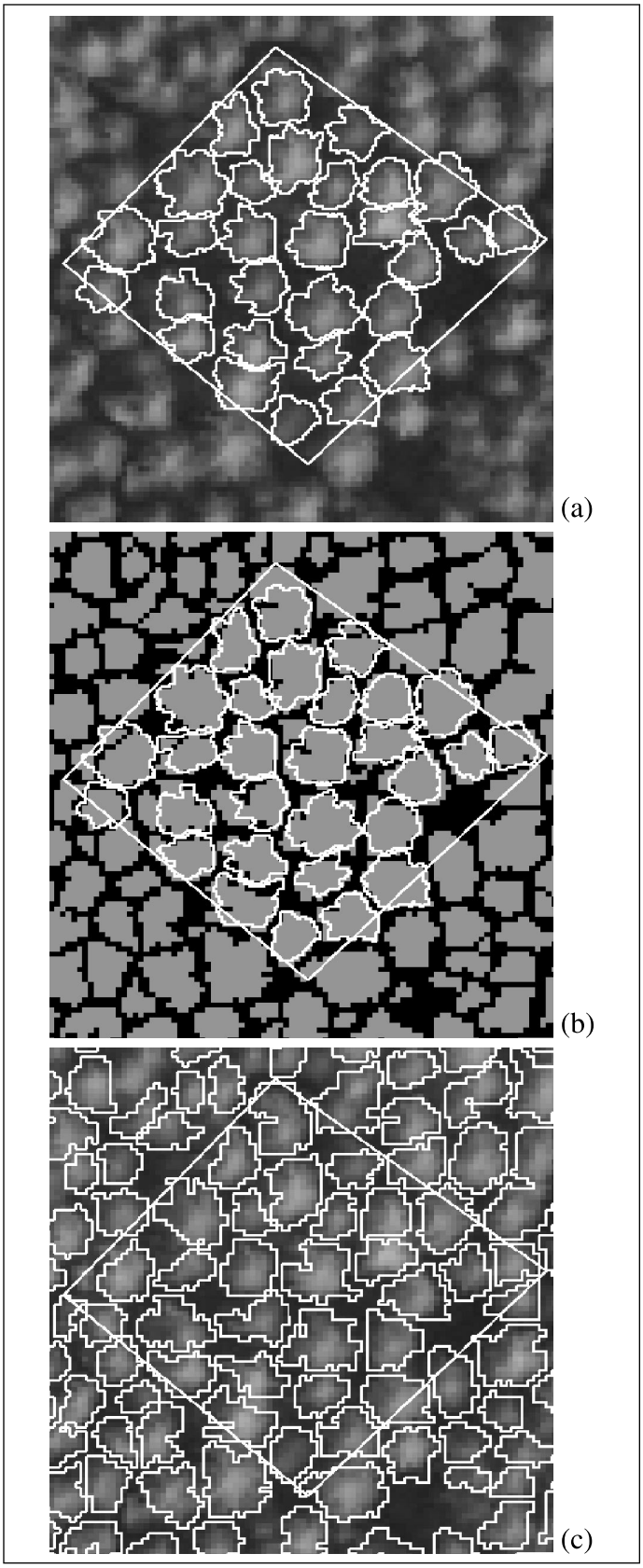

Figure 4. (a) Ground referenced delineations in plot 18 over digital frame camera orthoimage resampled to 50 cm/pixel. (b) Individual tree crown isolations (before height and size filtering) in bitmap format added to (a). (c) Resulting automatically delineated isols as polygons after the application of height and size filters. The 3 × 3 average filtered green spectral band used as input to the crown isolation process is shown in the background.

by the ground reference delineations are quantified versus these criterion. Results are analyzed in terms of how well the ground reference trees are represented by isols (gred-centric), as well as, how well each isol matches with the ground reference delineations (isol-centric). Commissions are an example of an isol-centric error.

Results

Tree crown isolation

Tree isolation with DFC imagery

Correspondence of automatically delineated trees with the ground reference trees was generally good (**Figure 4**). Over all three plots, 80% of the ground reference delineations had corresponding isols that were considered perfect matches and another 5% had good matches (**Table 2**). Of these matches, the isols were generally of similar size to the ground reference delineations. The open plot (plot 19) had the least percentage of perfect matches and the densest plot (plot 18) the highest. Splitting of trees into several isols was a main source of error, but nevertheless it was not a large problem. The split trees were all cases of a ground reference tree being split into only two isols and one of the isols had a predominant match. The other isol occupied less than 20% of the area of the ground reference delineation and was generally smaller. Commissions, isols not associated with a tree, however, were a problem.

Commission error was large for the open plot (53% of all isols were commissions). There were only five and four commission isols for plots 20 and 18, respectively, which was 18% and 11% of all isols in the plots. The sunlit ground in the gaps between trees formed image intensity structures that were considered isols. A spectral filter is often used to eliminate these spurious isols in open areas as they are often associated with nonvegetated surfaces or spectrally different vegetation. However, they cannot always be successfully filtered in this way. The size filter applied to the isols (i.e., eliminating isols < 7 m^2) worked well since many of the commissions were small in size and for the study area, trees were all of moderate size. The number of commissions was greatly reduced (to four for plot 19 and one each for plots 20 and 18). All the split cases became perfect matches, as the nondominant isol of the split cases was always small. As well, a case of a good match with a dominant isol and a secondary isol only minorly associated with it, became a perfect match.

The laser data were also used to help eliminate spurious isols. Any isol with a maximum height of less than 2 m was rejected as a tree crown isolation. This reduced the number of commission isols to nine, four, and four for plot 19, 20, and 18, respectively. Only commission isols were affected, the results for the other isolations remained the same. Reduction was

Figure 5. (a) Ground referenced delineations in plot 18 over canopy height model (CHM) image resampled to 50 cm/pixel. (b) Individual tree crowns isolations (before height and size filtering) in bitmap format added to (a). (c) Resulting automatically delineated isols as polygons after the application of height and size filters. The 3 × 3 average filtered CHM used as input to the isolation process is shown in the background.

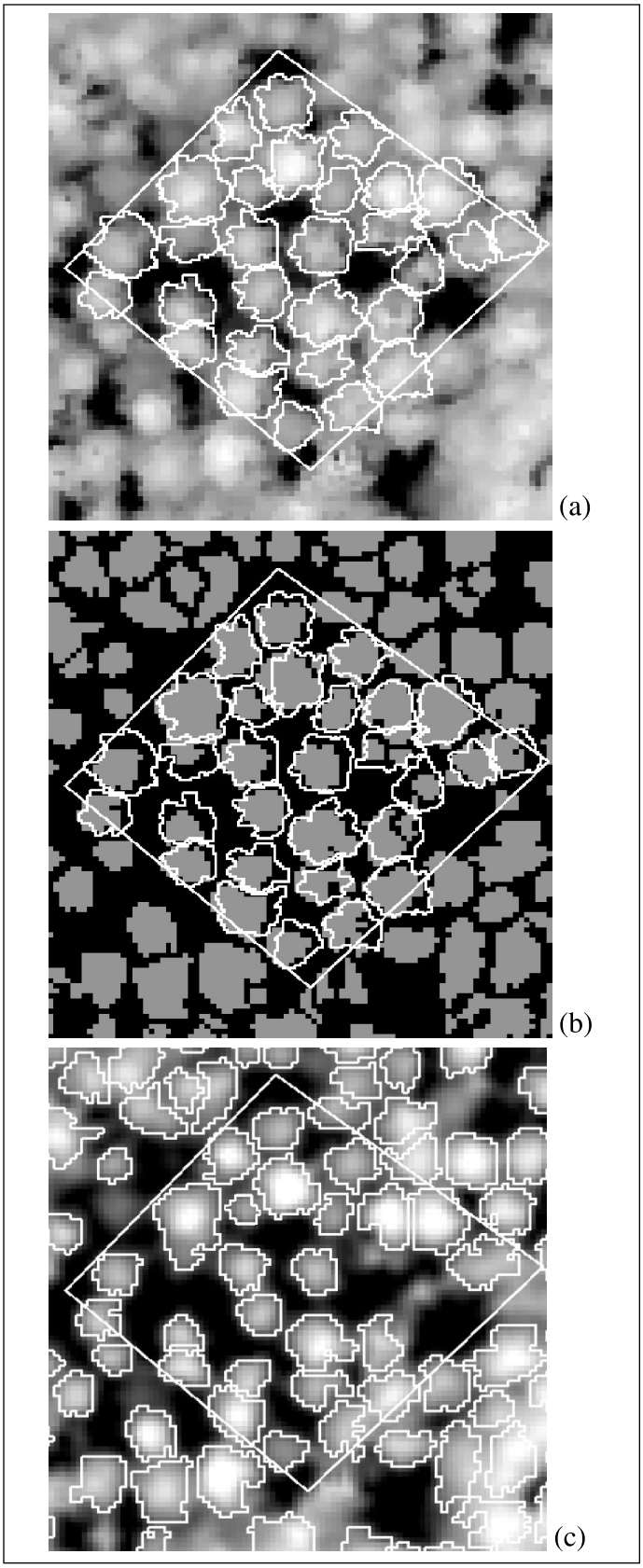

Table 2. Correspondence of automated tree crown isolations versus ground reference trees for the DFC imagery.

Plot	Match type				Commission	Total	Total
no.	Perfect	Good	Split	Poor	isols	greds	isols
19	7	3	1	1	17	12	32
20	16	0	3	1	5	20	28
18	26	0	3		4	29	36
Total	49	3	7	2[a]	36	61	96

Note: Number of ground reference trees of each type of match and number of commission isols are given.

[a]Nil trees omitted or incorporated into an isol associated with another ground reference tree.

mainly on the open plot. On the densest plot (plot 18), no isols were removed. For those commission isols not removed, most had heights between 4 and 20 m and all but four were under 7 m^2 in area. Four commission isols were >7 m^2 and had heights in the order of the actual tree heights.

Invoking both the height and size criteria produced much reduced commission errors and some improvements in terms of the split and good matches (**Table 3**). Almost all commission errors were removed. Ninety-seven percent of the ground reference trees had a perfect or good match. Results (after the commission filtering) were also examined from the point of view of how well each isol represents a tree (i.e., isol-centric). Of all remaining isols, 89% were considered a good or better match with a gred (86% were perfect matches), 5% were poor matches with a gred, and 6% were commissions.

Tree isolation with lidar imagery

Isolation of trees in the open and moderate density plots was good, being approximately similar to the DFC results (**Table 4**). Unlike the DFC imagery, however, commissions were not a problem. There was a lower percentage of perfect matches (59%) and more poorly represented trees (28%) for the densest plot (plot 18). The split ground reference delineations were all divided into only two isols and one was always dominant. There were three cases of poor matches where two manual trees had the same isol most associated with it. The isols derived from the CHM were often smaller than the ground reference delineation and corresponding DFC imagery isolations. Evaluating all the isols, 67% were considered a good or better match with a gred (60% were perfect matches), 12% were involved in split trees, 15% were poor matches with a gred, and 6% were commissions.

Height and size filtering improved results (**Table 5**). The height filtering did not remove any isols. The size filtering eliminated no isols from the open plot, four from plot 20, and seven from the densest plot (plot 18). This reduced commission error and split cases to nil. The situation is more complex in plot 18. One good isolation was eliminated by the filtering and

Table 3. Correspondence of automated tree crown isolations versus ground reference trees for the DFC imagery after a crown size filter and a height filter were applied to the isols.

Plot no.	Match type				Commission isols	Total greds	Total isols
	Perfect	Good	Split	Poor			
19	9	2	0	1	2	12	15
20	19	0	0	1	1	20	21
18	29	0	0	0	1	29	30
Total	57	2	0	2[a]	4	61	66[a]

Note: Number of ground reference trees of each type of match and number of commission isols are given.

[a]Nil trees omitted or incorporated into an isol associated with another ground reference tree.

Table 4. Correspondence of automated tree crown isolations versus ground reference trees for the lidar generated digital height model imagery.

Plot no.	Match type				Commission isols	Total greds	Total isols
	Perfect	Good	Split	Poor			
19	8	2	0	2	0	12	12
20	16	1	2	1	2	20	25
18	17	2	2	8[a]	2	29	32
Total	41	5	4	11[a]	4	61	69

Note: Number of ground reference trees of each type of match and number of commission isols are given.

[a]Three of the poorly matched trees were incorporated into an isol associated with another ground reference tree.

Table 5. Correspondence of automated tree crown isolations versus ground reference trees for the lidar generated digital height model after a crown size filter and a height filter were applied to the isols.

Plot no.	Match type				Commission isols	Total greds	Total isols
	Perfect	Good	Split	Poor			
19	8	2	0	2	0	12	12
20	17	2	0	1	0	20	20
18	18	1	0	9[a]	0	29	25
Total	43	5	0	13[a]	0	61	57

Note: Number of ground reference trees of each type of match and number of commission isols are given.

[a]One tree omitted and three of the poorly matched trees were incorporated into an isol associated with another ground reference tree.

became an omission. Both before and after size filtering, three isols had two manual trees most associated with them. Two of these cases had second or third isols associated with the second manual tree. These secondary isols were eliminated by the size filtering. The net result therefore was that four trees were not identified as separate entities. One was completely missed (omitted), whereas the other three were at least partially incorporated into an existing isol. There were just a few changes to other cases. Over all three plots, the number of perfect, good, and poor matches was 43, 5, and 9, respectively, accounting for 70%, 8%, and 15% of the ground reference trees. Filtering did not increase the number of good matches greatly (75% to 79%); there was a trade off between eliminating small isols, thus reducing the number of split trees and causing omissions. From an isol-centric perspective, 84% of all isols were good matches with ground reference delineations, 16% were poor, and there were no commissions.

Overall, if commission errors are excluded, the actual crown delineations of the DFC imagery appear to be a better representation of the crown boundary than those from the lidar data (e.g., **Figure 4** versus **Figure 5**). Including commission errors, the lidar appears to work best for lower densities, and the optical imagery works best for the denser plots.

Individual tree crown heights

Heights for DFC ground reference delineations

Examination of the heights derived from the lidar data for the manually delineated ground reference trees indicates the effectiveness of the lidar data for tree height extraction without complication caused by error in the automated isolation process. The heights determined for each ground reference delineation were very similar whether one used the highest laser hit within the gred or the highest point of the surface model within the gred. Eighty percent of the heights from the CHM and lidar hits were within ±0.5 m of each other, while five of 61 trees had CHM-derived heights that were >1 m different (all higher) than height estimates from the highest lidar hit. On average, the maximum tree elevation was 0.24 cm higher using the maximum of the CHM versus the highest laser hit within the gred.

There was an average underestimate of ground measured tree height by 1.32 m (standard deviation (SD) 0.81) for the CHM maximum and 1.56 m for the maximum lidar hit (SD 0.77). Only six trees had CHM maximum height estimates higher than the ground height; only one maximum lidar hit height was higher than the actual tree. Although the site has limited range of tree heights, a regression of lidar versus ground measured height for the greds indicates the underestimation but a good relationship (**Figure 6**).

Lidar heights were also compared with the height to the last (highest) whorl. It was thought that the true top of the trees, usually being a single leader branch, would have insufficient reflecting surface and structure to cause a lidar return strong enough to be recorded as the first return. However, the last whorl with usually three or four branches can cause sufficient lidar return and thus form a reference height representing the elevation in the canopy from which the first return comes from. The distance from the top of the leader to last whorl averaged 37 cm and reduced the height underestimate by this amount. The last whorl, however, did not represent the reference location on the crown that was the source or elevation of the first lidar return for this data set. The height generated from the lidar CHM relative to the ground measured height to the top of the leader will be used as the primary analysis of height for the automated tree isolations.

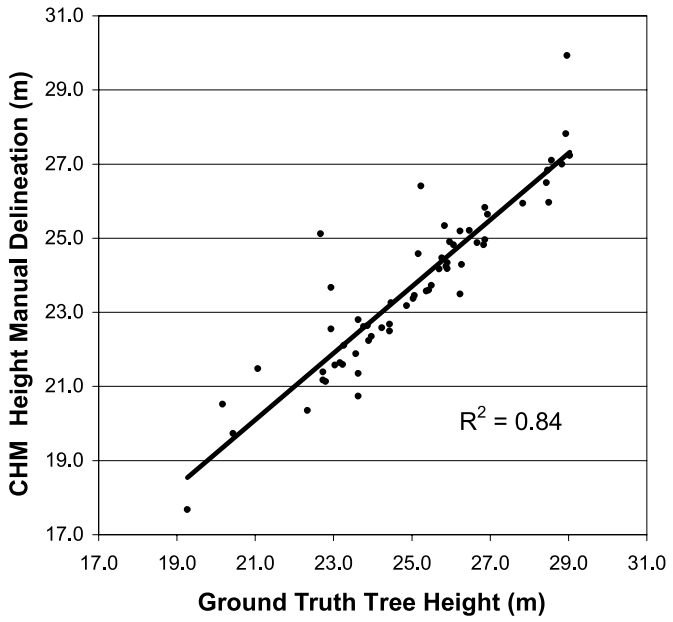

Figure 6. Heights of ground reference delineations determined from canopy height model (CHM) relative to field measured heights.

Heights for DFC automatic isolations

For those ground reference trees having an isol with a good match, heights were generally within –0.6 to –2.0 m of the tree height. Plot 18 had five isols with heights slightly higher than that of the ground reference trees (0–1 m). In addition, one isol had a height 2.4 m higher than the associated ground reference tree because it was slightly overlapping with a portion of the CHM related to another higher tree. Mean error was –1.23 m with a SD of 0.87, indicating a consistent underestimation of tree height (**Figure 7**). The poor isolations produced poorer height estimates, one being –1.7 m and the other –2.7 m. For split trees, the heights of the dominant isol were as accurate as the perfect and good matches. However, the second isols did not capture the peak of the tree crown and had maximum CHM heights of typically 3.5 to 10 m (average –6.5 m) below that of the ground reference tree. It is also interesting to note that for the committed isols (i.e., isols with no associated gred) many of the heights were close to zero.

The size and height filtering process eliminated all secondary isols associated with split cases and most of the commission errors. For the ground reference trees with a good isol match, average height error was –1.27 m (SD 0.92). However, even after filtering, four committed isols remained plus one secondary isol minorly associated with a ground reference tree that also had a dominant isol. Therefore, if one was counting trees and tallying total heights, there were five isols (trees) with heights in the range of the actual trees, that really did not exist. If these five isols were not included, average height estimation error of the isols regardless of quality of match was –1.30 m. **Table 6** summarizes the average height of the plots if all isols (after height and size filtering) were included regardless of type of match. There was no notable trend of greater or less height error between plots of different densities.

Height for lidar isolations

Ground reference delineations with a good match with an isol had an average height error of –1.45 m (SD 0.69), with most errors between –0.8 and –2 m. Isols with a poor match had better height estimates than the poor isolations of the DFC imagery. Underestimation was similar to the good matches, but several had a slight overestimate. As with the DFC imagery isolation, the dominant isol in split cases had similar error as the isols with good matches, and the secondary isols had larger underestimations (average –4.9 m).

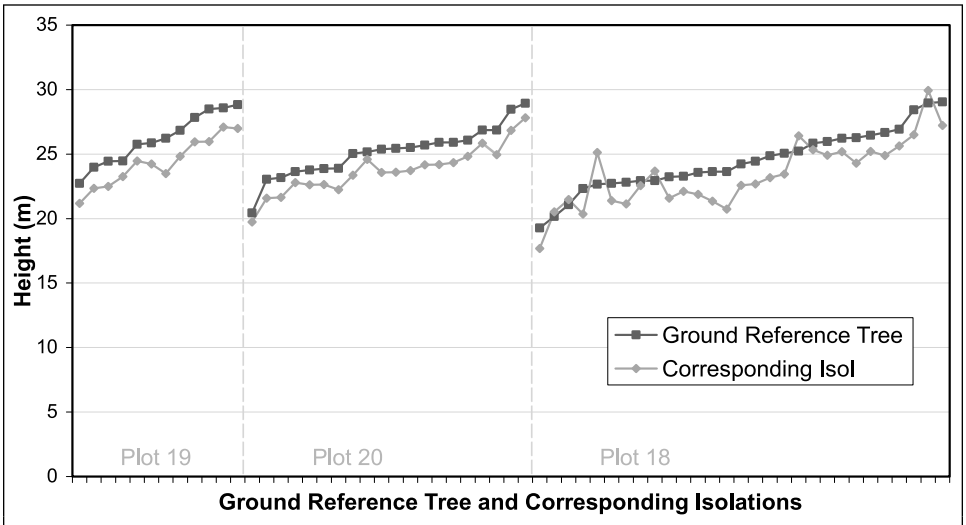

Figure 7. Heights of the ground reference trees relative to the height derived from the automatically delineated tree crown (isol) most associated with it (from the digital frame camera image analysis after height and size filtering). Trees within each plot are ordered according to height.

Table 6. Comparison of average plot stems/ha and height from all isols after filtering for the digital frame camera (DFC) imagery and lidar canopy height model (CHM) isolations versus the average of the ground measured trees.

Plot no.	Feature	Ground data	DFC imagery	Lidar CHM
19	Density (stems/ha)	300	375	300
19	Height (m)	26.2	23.5	24.4
20	Density (stems/ha)	500	525	500
20	Height (m)	25.2	23.5	23.9
18	Density (stems/ha)	725	750	650
18	Height (m)	24.4	23.3	23.6
Total[a]	Density (stems/ha)	508	550	483
Total[a]	Height (m)	25.0	23.5	23.8

[a]Total over all three plots.

After filtering, there was no commission error or split trees, but there was one omission and three trees secondarily associated with isols that had their main correspondence with another tree. Average height error of isols versus the height of their most associated ground reference tree was –1.33 m. This does not account for the omitted tree that has no height associated with it and the three trees secondarily associated with isols. Several of the poor match isols had positive height differences. The average error in height estimation for ground reference trees with a good match isol was –1.44 with SD 0.68. Average height over all filtered isols of any type was 1.2 m below the average height of all ground reference trees (**Table 6**). Apart from the poorer and more complex isolation on the densest plot (plot 18), there was no trend of height error at the tree level with plot density.

Discussion

Crown isolation — multispectral imagery

Automated isolation of individual tree crowns on the DFC imagery with the valley following approach produced results in keeping with other studies. The method utilizes the shaded areas in gaps between trees and the intensity pattern of bright areas near the apex of the crown and lower image intensities at the edges of trees or where trees meet. The technique therefore works well for moderate density conifer stands (Gougeon, 1995a; Andrew et al., 1999; Leckie et al., 1999a). Isolations for the stands of this study corresponded well with the ground reference trees; 80%–90% of the ground reference trees had good matches with an isol. Results were better on the denser plot of this study. However, poor results are expected at high densities such as those of the control plots of the LOGS study site (2000 stems/ha). When sunlit open areas occur especially in forest gaps, many features can produce a similar image intensity pattern as a tree. Thus in open stands commission errors can become a problem. Spectral filters are usually effective for eliminating these, especially for nonvegetated features. For ground vegetation, shrub, or understory, such filters can have difficulties and commissions remain a problem. Commission errors were large for the open stand (plot 19). In this study it has been shown that a simple height filter derived from the lidar data applied to the isols was effective at eliminating spurious isols generated from sunlit ground vegetation. It may be less effective when there is a range of heights of exposed canopy trees from close to the ground to tall. A size filter was also useful for both commissions and split trees, but will not be so if tree sizes vary and are small. It is difficult to create good tree isolations when tree sizes differ without omitting or combining trees or splitting large trees into several isols. For the plots of this study, crown sizes were similar and splitting of crowns occurred but was minor. After filtering, split crowns were eliminated, 97% of the ground reference trees had a good or better match with an isol, commission errors were 6%, and 89% of the isols had a good match with the ground reference delineations.

Crown isolation — canopy height model (CHM)

The valley following approach to tree crown isolation should be effective when applied to the digital height model. It basically uses the image intensity as a surrogate for hill and valley terrain, the peaks being trees and valleys the gaps or join between them. This is the type of three-dimensional topography formed by the canopy envelope of trees. Results of this study are a first application of the valley following technique to such high-density lidar data and do not necessarily represent optimum solutions. Nevertheless, comparison with the ground reference delineations showed good correspondence (75% of the ground reference trees had good matches). Before height and size filtering, omissions were nil and commissions low. Accuracy was less for the dense plot (84% good matches for the low and moderate density plots (plots 19 and 20), 66% for the denser plot (plot 18)). Results are expected to degrade for even denser cases. It was speculated that the detailed three-dimensional structure afforded by the high-density lidar data might help resolve tree crowns in dense situations where the optical methods have difficulties. These results indicate that this may not be the case. There were slightly fewer split trees on the lidar generated isols, but it is not conclusive that the lidar data will help reduce splitting of larger trees. The process of using the CHM for isolation was effective in not capturing isols in open areas. The original commission error was low and the height filter did not eliminate any further isols. The size filter however was effective. When applied to the lidar generated isols, both commission error and split tree cases were eliminated completely. However, it did create several missing trees, either omitted or partially included in an isol mostly associated with another tree. After filtering, the percentage of good matched ground reference trees over all plots was 79%, and 84% of all isols had a good match with a gred.

Although there have not been a large number of studies automatically isolating trees and tree boundaries with lidar data, good detection of trees has been achieved. Hyyppä et al. (2001) showed variable results over different conditions but on average 50% isolation success, and found poorer capabilities

for closely spaced interlocking crowns. In another study, tree detection using an automated tree crown segmentation approach resulted in varying detection depending on tree size but generally 80%–90% of the larger trees were detected (Persson et al., 2002). No other study has used the valley following approach and analyzed tree detection in terms of crown outlining accuracy, so it is interesting that this approach also produced good results in terms of tree detection and provided reasonable crown outlines for most trees.

Crown isolation — crown outline

The actual outline, size, and shape of the isols associated with ground reference trees (i.e., excluding commissions and omissions) generated from the lidar CHM were not as well matched with the ground reference delineations as for the DFC imagery. This may partly be a consequence of the ground reference delineations being created on the DFC imagery, but regardless the outline of the trees did not appear as good. The CHM itself was generated by standard software used to produce DEMs of terrain. There are facets visible on the surface that correspond to sides of trees. The edges of the tree on the CHM are smoothed in the vertical dimension whereas in reality they are often breaklines. For example, for the trees of this study, the height to live crown was typically 9 m and the height surface should drop this distance to the ground at the edge of the crown. There were remaining holes in the canopy that the surface model creation process did not eliminate. This caused anomalies in the shape of the tree surface. All these factors contributed to the small crown size and inaccuracies in automated crown outlines.

Crown isolation — possible improvements

Improved crown isolation using lidar data and indeed height estimation results might be expected with better methods of generating the CHM that specifically take into account the expected shape of the surface within a forest canopy. Smaller lidar footprint size, even spacing between laser hits, and data acquisition from one flight line instead of multiple lines would also improve results. Refinements and further exploration of the valley following approach should be undertaken. For example, using expected height to live crown to stop and start the valley generating process would be useful.

Further improvements might be expected by using local maxima techniques to help the isolation process. These techniques find local maxima within a given window and these are often associated with tree crowns. This could be used to confirm presence of a crown and eliminate some of the split cases and commissions. The template matching approach should be effective on the CHM. A three-dimensional shape model would be produced for various crown configurations and the CHM searched for good matches, much as is done with template matching methods for optical imagery. The models can be modified to reflect different view angles of the lidar data. Indeed, such models themselves could be used to create an individual crown shape tailored for each crown and the height from this model may prove a better measure of the actual tree height than the general CHM beneath that tree. The details of these methods and how to combine them needs study, development, and testing.

View angle causes difficulties with tree isolation on both the lidar and optical imagery, and narrow fields of view are preferable. Different parts of the crown and crown outlines are visible depending on view angle. On optical imagery, a tree looks quite different at nadir than it does from the sunlit side, and can be quite different again when viewed from the shaded side. This study used data from the portion of individual DFC frames near nadir (plot 19 was at the highest view angle, 22° at the center of the plot). Orthocorrection of imagery at larger view angles can produce anomalous looking trees. Full orthomosaicking of many individual frames with standard techniques can result in very peculiar trees at large view angles. As well, there can be trees missing and trees added twice at frame boundaries. If detailed single tree analysis is to be done using orthorectified mosaic imagery, then great care must be taken with the processing and perhaps new mosaicking routines developed.

Individual tree heights — causes for underestimations

At the density of lidar hits and footprint size of this data set, there should be complete coverage of the entire area by a laser signal. The consistent underestimate in tree height is therefore not likely due to the laser coverage not hitting the tops of the trees. It could be related to a lack of lidar reflection off the top of the tree or the threshold at which the sensor detects a return signal. There is an underestimate even when the laser derived height is compared with the height of the last whorl where there are several branches to provide reflecting surfaces that might give a signal large enough to form the first return. Alternately, the ground surface of the study plots typically had dense salal of 0.5 to 1.1 m in height and patches of bracken of varying density up to 2 m high. This could account for some of the 1.3 m height underestimate to the top of the tree leader and much of the 1 m underestimate of height to the last whorl (underestimates based on the height of the tree using the CHM). As well, the ground surface microrelief of the site could easily vary by 0.5 m (up or down) from the ground elevation at the base of the tree where the height was measured to the elevation of the general terrain the lidar ground surface model is representing. The reasons for the few overestimates of tree height based on the ground reference delineations are unknown. There is a need to determine the cause and nature of the inherent underestimation in individual tree heights. For example, a study examining individual tree height estimations in terrain with a simple flat solid ground surface could determine at what distance into the tree structure or along a tree surface envelope a first-return response comes from for different shaped trees, footprint sizes, and first-return instrument thresholds.

The 1.3 m underestimation of height with a SD of 1.0 is within requirements for forest inventory. The inventory

underestimation of tree height can be compensated for with regression techniques. Other studies have produced varying results for tree height estimation, but have generally been good. Næsset and Økland (2002), examining lidar with a spacing of 0.7 to 1.3 m and using laser hits within ground surveyed crown outlines, did not produce good individual tree height estimates even with regression techniques, although mean heights over the stand were good. Persson et al. (2002) automatically identified tree crowns on high-density laser data and also determined a negative offset (1.1 m) and very good tree height estimation (root mean square error from the regression of 0.63 m). Hyyppä et al. (2000) again using regressions also produced good tree heights (standard error 0.97 m) and did not have a negative offset (only a –0.14 m offset). Using tree isolation and high-density lidar data to extract stand parameters, Hyyppä et al. (2001b) estimated mean stand height to a 1.8 m standard error.

Individual tree heights — use of CHM versus highest laser hits within crown isolations

Theoretically, the CHM should produce better tree height estimates than the laser hits themselves. The model should project the tree surface shape to the peak of the crown. A hit at the peak or signal from the very top of the crown is not necessarily needed. The data of this study indeed did show heights from the CHM to be slightly higher and closer to true tree heights than those derived from the highest laser hit within the automated isolation (on average 0.24 cm). However, the DEM algorithm used to generate the CHM is not designed for the peaked shape of trees and this theoretical advantage may not be fully realized. For deciduous trees, which are not necessarily peaked, the effectiveness of the current DEM generation methods may be better, but still needs investigation. Smaller footprint size may also improve the CHM over trees. Data acquisition in one pass rather than multiple passes would eliminate the main source of canopy "holes" and improve the CHM, and also provide a self-consistent set with no possibilities for misregistration errors among the data from different flight lines. However, if a single pass is used, a narrow field of view is desirable to prevent lidar shadowing (i.e., lack of hits on the side of the trees opposite the viewing direction).

Heights on a stand basis — combined effect of isolation and tree height underestimation

The combined influence of tree isolation and lidar height estimation is dependent on the accuracy of the height estimation (once a good isolation is achieved) and the quality of the tree isolations. It appears that there is likely an inherent underestimation of tree height with the laser data. This was –1.3 m for the ground reference delineations and, as mentioned above, may be partly related to ground vegetation and microrelief. The automated isolations for the trees with a good match captured the main part of the tree crown that included the highest point on the tree. Perfect matches did not produce better heights than the good cases with only one associated isol. There was no trend of better heights for individual trees with the different plot densities of this study. The dominant isol in cases where trees were split into two isols also captured the highest point on the tree. For cases with good matches, because of good correspondence, the heights derived from the manually delineated and automated DFC or CHM crown isolations were similar and usually the same. Variations between the average results for CHM- and DFC-derived good matches are therefore more related to which trees were good matches rather than better capabilities of the isolations on each medium. Poor isolations had varied height errors but were generally between –3 and –5 m for the DFC data and usually less for the lidar-generated isols. Their influence on overall height estimates for a stand will depend on the number of these poor isolations. For the stands of this study, the number of poor cases was small and did not have a large effect on the overall height estimates (**Table 6**). Commissions and cases of single isolations representing parts of two trees are likely the most serious source of error. For the stand conditions and isolations of this study, these types of isolation errors were small after height and size filtering. As well, the remaining commission isols had heights in the range of the actual trees of the stands. For the lidar isolations, there were three cases of a single isol covering parts of two trees not represented by any other isols. In these cases the heights of the trees were similar, and the height estimations from the isols represented both trees well. Therefore, stand averages were not greatly affected even though some additional trees were created and others were essentially omitted (**Table 6**).

Synergy of optical imagery and lidar

There is a synergy between the high resolution optical imagery and lidar data sources for producing forest inventory information. Combination of high-resolution spectral imagery and laser data for automated individual tree crown analysis offers large potential benefits. A major limitation of the automated tree analysis of spectral imagery has been the lack of height information, an important information requirement. If high-resolution data from spectral imagers and lidar systems can be combined, individual tree height information may be extractable along with the species, health, and other tree attributes derived from the multispectral images. The two data sources can also be used to improve tree isolations.

Lidar appears capable of providing effective tree height data, whereas optical imagery can provide multispectral and spatial detail useful for species and health estimation. Both have capabilities, although somewhat different, for stem counts and locations, tree isolation, and crown closure or canopy gap estimation or mapping. The data of this study, although not covering a large range of conditions, indicated that optical data may be better at outlining crowns in denser situations and thus be given more weight in these situations. After size filtering, lidar tree isolation results were good, but there were omissions that did not occur with the optical imagery. To gain forest inventory information on tree species or health, a crown outline

related best to the optical data is preferable. Therefore, even if the lidar data produced better stem counts or outlines for heights, the outline from the optical imagery may be used for species or health classification.

Tree isolation algorithms using panchromatic or multispectral imagery often have difficulty when stands are dense and tree crowns interleaved. The intensity pattern is not distinct. It was thought that there may be structure in the canopy envelope represented on the lidar data that helps separate these crowns. This was not the case for the data set and forest conditions of this study, indeed the multispectral data separated trees better in the densest plot (725 stems/ha). Results are expected to start to degrade for both the multispectral and lidar data for higher densities.

For large crowns, individual large branches can cause the algorithms to split trees into several entities. It is especially difficult to parameterize the algorithm to produce good results where there is a mixture of crown sizes. Again the three-dimensional shape provided by high-density lidar data might be expected to not represent the branches as distinct structures and perhaps prevent tree splitting by tree crown isolation algorithms. This was partially true, but both data sets suffered somewhat from tree splitting. A size filter helped eliminate this problem.

In open stands there are often structures in the spectral images that may be mistaken for trees (e.g., shrub vegetation or clumped ground vegetation). Applying a height filter from the lidar data reduced greatly such commission errors on the multispectral data. This was also noted by Gougeon et al. (2001). Schreier et al. (1985) also showed the value of combined reflectance and height data by separating treed vegetation from ground vegetation using both laser intensity and height information.

Much more exploration of the advantages and disadvantages of the different data sources in different forest conditions is needed, as well as development of methods to combine the data sources and analyses.

Conclusions

This study has shown that with existing sensor and processing systems, a high-density combined multispectral and lidar data set suitable for individual tree crown isolation and tree height measurement can be created. Data acquisition parameters for both the imagery and laser data need to be tailored to this purpose. High-density data acquisition and processing must become more routine. Preprocessing to eliminate holes in the canopy without altering the ground hits at the edge of trees needs development. Standard DEM generation techniques need improvement for this application, and perhaps specialized methods developed that take into account the three-dimensional shapes expected in a forest canopy.

There is a strong synergy among the two data sources — optical imagery and high-density lidar data. Each did well on its own, but had weaknesses that were partially alleviated by the other. For example, the lidar easily eliminated most of the commission errors that often occur in open stands with optical imagery, whereas the DFC data produced a better isolation in the more dense stands. The valley following tree isolation approach by its nature should do well with optical imagery for moderately dense conifer stands as well as with lidar data. More investigation with similar lidar data over a wider set of densities and forest types is needed. Other techniques like local maxima and template matching could add further information to improve the tree isolation. The use of three-dimensional shape, two-dimensional tree outline shape, and perhaps three-dimensional texture should be explored for use in helping with species identification.

Sources of the underestimate of tree height were examined, but a conclusive cause cannot be ascribed from this data set. However, it is expected that regardless of any improved method, there will still be a small negative offset for the tree height as measured to the top of the leader. Once its specific cause and relation to tree species or structure are understood, it is anticipated that the offset can be compensated for theoretically or empirically.

The concept of combining high-resolution imagery and dense lidar data for individual tree crown analysis has been presented and a simple demonstration and test conducted. For a set of 55-year-old conifer stands of varying density (between 300 and 725 stems/ha), the combination of the two data sets gave good tree isolations and heights that were estimated (underestimated) to within 1.3 m. This represents a simple and limited set of forest conditions and further testing is needed. There remains a series of research and development challenges and operational and cost issues to be resolved, but results show that these are worth pursuing and that such a concept is a viable forest survey tool.

Acknowledgements

Thanks go to Dennis Beddows, Donna Macey, and many others who developed and maintained LOGS sites for the Canadian Forest Service. Robert Jordan and William Burt assisted with field data collection and compilation. Many staff members at Terra Remote Sensing Inc. contributed through data acquisition and processing.

References

Aldred, A., and Bonnor, M. 1985. *Application of Airborne Lasers to Forest Surveys*. Canadian Forestry Service, Petawawa National Forestry Centre. Information Report Pl-X-51. 62 p.

Andersen, H.-E., Reutebuch, E.S., and Schreuder, G.F. 2001. Automated individual tree measurement through morphological analysis of a lidar-based canopy surface model. In *Proceedings of the First International Precision Forestry Symposium*, 17–20 June 2001, Seattle, Wash. College of Forest Resources, University of Washington, Seattle, Wash. pp. 11–22.

Andrew, R.M., Trotter, C.M., Höck, B.K., and Dunningham, A. 1999. Inventory of plantation forests using crown delineation techniques. In *Proceedings of the Fourth International Airborne Remote Sensing Conference and Exhibition – 21st Canadian Symposium on Remote*

Sensing, 21–24 June 1999, Ottawa, Ont. ERIM International Inc., Ann Arbor, Mich. Vol. 1, pp. 131–138.

Baltsavias, E.P. 1999. Airborne laser scanning: existing systems and firms and other resources. *ISPRS Journal of Photogrammetry and Remote Sensing*, Vol. 54, pp. 164–198.

Beddows, D. 2002. *Levels-Of-Growing-Stock Cooperative Study in Douglas-fir: Report No. 16 – Sayward Forest and Shawnigan Lake*. Pacific Forestry Centre, Canadian Forest Service, Natural Resources Canada, Victoria, B.C. Information Report BC-X-393. 67 p.

Chappelle, E.W., and Lichtenthaler, H. (Editors). 1994. Special issue on fluorescence measurement of vegetation. *Remote Sensing of Environment*, Vol. 47, pp. 1–105.

Crown, M., and Brett, C.P. 1975. *Fertilization and Thinning Effects On a Douglas-fir Ecosystem at Shawinigan Lake – An Establishment Report*. Pacific Forest Research Centre, Canadian Forestry Service, Natural Resources Canada, Victoria, B.C. Report BC-X-110.

Culvenor, D.S. 2002. *TIDA: an algorithm for the delineation of tree crowns in high spatial resolution digital imagery of Australian native forest*. Ph.D. thesis, University of Melbourne, Melbourne, Australia.

Dralle, K., and Rudemo, M. 1997. Stem number estimation by kernel smoothing of aerial photos. *Canadian Journal of Forest Research*, Vol. 26, pp. 1228–1236.

Dubayah, R., Blair, J.B., Bufton, J.L., Clark, D.B., JaJa, J., Knox, R., Luthcke, S.B., Prince, S. and Weishampel, J. 1997. The vegetation canopy lidar mission. In *Proceedings of the ASPRS Conference on Land Satellite Information in the Next Decade II: Sources and Applications*, 5–7 December 1997, Washington, D.C. American Society for Photogrammetry and Remote Sensing, Bethesda, Md. pp. 100–112.

Gougeon, F.A. 1995a. A crown-following approach to the automatic delineation of individual tree crowns in high spatial resolution aerial images. *Canadian Journal of Remote Sensing*, Vol. 21, No. 3, pp. 274–284.

Gougeon, F.A. 1995b. Comparison of possible multispectral classification schemes for tree crowns individually delineated on high spatial resolution MEIS images. *Canadian Journal of Remote Sensing*, Vol. 21, No. 1, pp. 1–9.

Gougeon, F.A. 2000. *Towards semi-automated forest inventories using individual tree crown (ITC) recognition*. Pacific Forestry Centre, Canadian Forest Service, Natural Resources Canada, Victoria. B.C. Technology Transfer Note – Forestry Research Applications, No. 22. 6 p.

Gougeon, F.A., and Moore, T. 1989. Classification individuelle des arbres à partir d'images à haute résolution spatiale. In *6e Congrès de l'Association québécoise de télédétection*, 4–6 May 1988, Sherbrooke, Que. L'Association québécoise de télédétection, Sainte-Foy, Que. pp. 185–196.

Gougeon, F.A., St-Onge, B.A., Wulder, M., and Leckie, D. 2001. Synergy of Airborne Laser Altimetry and Digital Videography for Individual Tree Crown Delineation. In *Proceedings of the 23rd Canadian Symposium on Remote Sensing – 10e Congrès de l'Association québécoise de télédétection*, 21–24 August 2001, Sainte-Foy, Québec. Canadian Aeronautics and Space Institute, Ottawa, Ont. [CD-ROM].

Haara, A., and Nevalainen, S. 2002. Detection of dead or defoliated spruces using digital aerial data. *Forest Ecology and Management*, Vol. 160, pp. 97–107.

Harding, D.J., Lefsky, M.A., Parker, G.G., and Blair, J.B. 2001. Laser altimeter canopy height profiles: methods and validation for closed-canopy, broadleaf forests. *Remote Sensing of Environment*, Vol. 76, pp. 283–297.

Hill, D., and Leckie, D.G. (Editors). 1999. *Proceedings of the International Forum on Automated Interpretation of High Spatial Resolution Digital Imagery for Forestry*, 10–12 February 1998, Victoria, B.C. Pacific Forestry Centre, Canadian Forest Service, Natural Resources Canada, Victoria, B.C. 402 pp.

Hyyppä, J., Psysalo, U., Hyyppä, H., and and Samberg, A. 2000. Elevation accuracy of laser scanning-derived digital terrain and target models in forest environment. In *Proceedings of the Fourth EARSeL Workshop on Lidar Remote Sensing of Land and Sea*, 16–17 June 2000, Dresden, Germany. pp. 139–147.

Hyyppä, J., Schardt, M., Haggrén, H., Koch, B., Lohr, U., Scherrer, H.U., Paananen, R., Luukkonen, H., Ziegler, M., Hyyppä, H., Psysalo, U., Friedländer, H., Uuttera, J., Wagner, S., Inkinen., M., Wimmer, A., Kukko, A., Ahokas, A., and Karjalainen, M. 2001a. HIGH-SCAN: The first Europoean-wide attempt to derive single-tree information from laser scanner data. *Photogrammetric Journal of Finland*, Vol. 17, pp. 58–68.

Hyyppä, J., Kelle, O., Lehikoinen, M., and Inkinen, M. 2001b. A segmentation-based method to retrieve stem volume estimates from 3-D tree height models produced by laser scanners. *IEEE Transactions on Geoscience and Remote Sensing*, Vol. 39, pp. 969–975.

Key, T., Warner, T.A., McGraw, J.B., and Fajvan, M.A. 2001. A comparison of multispectral and multitemporal information in high spatial resolution imagery for classification of individual tree species in a temperate hardwood forest. *Remote Sensing of Environment*, Vol. 75, pp. 100–112.

Larsen, M. 1997. Crown modeling to find tree top positions in aerial photographs. In *Proceedings of the Third International Airborne Remote Sensing Conference and Exhibition*, 7–10 July 1997, Copenhagen, Denmark. ERIM International Inc., Ann Arbor, Mich. Vol. II. pp. 428–435.

Leckie, D.G. 1990. Advances in remote sensing technologies for forest surveys and management. *Canadian Journal of Forest Research*, Vol. 20, No. 4, pp. 464–483.

Leckie, D.G., and Gougeon, F.A. 1999. An assessment of both visual and automated tree counting and species identification with high spatial resolution multispectral imagery. In *Proceedings of the International Forum on Automated Interpretation of High Spatial Resolution Digital Imagery for Forestry*, 10–12 February 1998, Victoria, B.C. Pacific Forestry Centre, Canadian Forest Service, Natural Resources Canada, Victoria, B.C. pp. 141–152.

Leckie, D., Smith, N., Davison, D., Jay, C., Gougeon, F., Achal, S., Burnett, C., Cloney, E., Lataille, S., Montgomery, F., Nelson, T., and Walsworth, N. 1999a. Automated Interpretation of High Spatial Resolution Multispectral (CASI) Imagery: A Development Project for a Forest Company. In *Proceedings of the Fourth International Airborne Remote Sensing Conference and Exhibition – 21st Canadian Symposium on Remote Sensing*, 21–24 June 1999, Ottawa, Ont. ERIM International Inc., Ann Arbor, Mich. Vol. II, pp. 201–211.

Leckie, D.G., Gougeon, F., Walsworth, N., Burnett, C., and Kent, G. 1999b. *Rules for Overlap Cases of Manually and Automatically Delineated Tree Outlines*. Internal Report. Canadian Forest Service, Natural Resources Canada, Victoria. B.C.

Lefsky, M.A., Cohen, W.B., Acker, S.A., Parker, G.G., Spies, T.A., and Harding, D. 1999. Lidar remote sensing of the canopy structure and biophysical properties of Douglas-fir western hemlock forests. *Remote Sensing of Environment*, Vol. 70, pp.339–361.

Lüdeker, W., Dahn, H.-G., Günther, K.P., and Schulz, H. 1999. Laser-induced fluorescence — a method to detect the vitality of Scots pines. *Remote Sensing of Environment*, Vol. 68, pp. 225–236.

MacLean, G.A., and Krabill, W.B. 1986. Gross-merchantable timber volume estimation using an airborne lidar system. *Canadian Journal of Remote Sensing*, Vol. 12, pp. 7–18.

Magnussen, S., and Boudewyn, P. 1998 Derivations of stand heights from airborne laser scanner data with canopy-based quantile estimators. *Canadian Journal of Forest Research*, Vol. 28, pp. 1016–1031.

Means, J.E., Acker, S.A., Harding, D.J., Blair, D.B., Lefsky, M.A., Cohen, W.B., Harmon, M.E., and McKee, W.A. 1999. Use of large-footprint scanning airborne lidar to estimate forest stand characteristics in the Western Cascade of Oregon. *Remote Sensing of Environment*, Vol. 67, pp. 298–308.

Næsset, E. 1997. Determination of mean tree height of forest stands using airborne laser scanner data. *ISPRS Journal of Photogrammetry and Remote Sensing*, Vol. 52, pp. 49–56.

Næsset, E., and Bjerknes, K. 2001. Estimating tree heights and number of stems in young forest stands using airborne laser scanner data. *Remote Sensing of Environment*, Vol. 78, pp. 328–340.

Næsset, E., and Økland, T. 2002. Estimating tree height and tree crown properties using airborne scanning laser in a boreal nature reserve. *Remote Sensing of Environment*, Vol. 79, pp. 105–115.

Nelson, R., Krabill, W., and Tonelli, J. 1988. Estimating forest biomass and volume using airborne laser data. *Remote Sensing of Environment*, Vol. 24, pp. 247–267.

Nilsson, M. 1996. Estimation of tree heights and stand volume using an airborne lidar system. *Remote Sensing of Environment*, Vol. 56, pp. 1–7.

Pinz, A. 1991. A computer vision system for recognition of trees in aerial photographs. In *Multisource Data Integration in Remote Sensing*. Edited by J. Tilton. International Association of Pattern Recognition Workshop, NASA Conference Publication 3099. pp. 111–124.

Persson, Å., Holmgren, J., and Söderman, U. 2002. Detecting and measuring individual trees using an airborne laser scanner. *Photogrammetric Engineering & Remote Sensing*, Vol. 68, pp. 925–932.

Pollock, R. 1996. *The Automatic Recognition of Individual Trees in Aerial Images of Forests Based on a Synthetic Tree Crown Model*. Ph.D. thesis, Department of Computer Science, University of British Columbia, Vancouver, B.C.

Popescu, S.C., Wynne, R.H., and Nelson, R.F. 2002. Estimating plot level tree heights with lidar: local filtering with a canopy-height based variable window size. *Computers and Electronics in Agriculture*, Vol. 37, pp. 71–95.

Pouliot, D.A, King, D.J., Bell, F.W., and Pitt, D.G. 2002. Automated tree crown detection and delineation in high-resolution digital camera imagery of coniferous forest regeneration. *Remote Sensing of Environment*, Vol. 82, No. 2–3, pp. 322–334.

Quackenbush, L.J., Hopkins, P.F., and Kinn, G.J. 2000. Developing forestry products from high resolution digital aerial imagery. *Photogrammetric Engineering & Remote Sensing*, Vol. 66, No. 11, pp. 1337–1346.

Saito, Y., Saito, R., Kawahara, T.D., Nomura, A., and Takeda, S. 2000. Development and performance characteristics of laser-induced fluorescence imaging LiDAR for forestry applications. *Forest Ecology and Management*, Vol. 128, pp. 129–137.

Schreier, H., Lougheed, J., Trucker, C., and Leckie, D. 1985. Automated measurements of terrain reflection and height variations using an airborne infrared laser system. *International Journal of Remote Sensing*, Vol. 6, pp. 101–113.

Tarp-Johansen, M.J. 2001. *Locating Individual Trees in Even-aged Oak Stands by Digital Image Processing of Aerial Photographs*. Ph.D. thesis, Royal Veterinary and Agricultural University, Copenhagen, Denmark. 158 pp.

Tickle, P.K., Witte, C., Lee, A., Jones, K., Denham, R., Lucas, R.M., and Austin, J. 2001. The use of airborne scanning lidar and large scale photography within an strategic forest inventory and monitoring framework. In *Proceedings of the IEEE International Geoscience and Remote Sensing Symposium, IGARSS 2001*, 9–13 July 2001, Sydney, Australia. IEEE Inc., Piscataway, N.J. [CD-ROM].

Trofymow, J.A., Porter, G., Blackwell, B., Arksey, R., Marshall, V., and Pollard, D. 1998. *Chronosequences for research into the effects of converting coastal British Columbia old-growth forests to managed forests: an establishment report*. Pacific Forestry Centre, Canadian Forest Service, Natural Resources Canada, Victoria, B.C. Information Report BC-X-374. 137 pp.

Uuttera, J., Haara, A., Tokola, T., and Maltamo, M. 1998. Determination of the spatial distribution of trees from digital aerial photographs. *Forest Ecology and Management*, Vol. 110, pp. 275–282.

Warner, T.A., Lee, J.Y., and McGraw, J.B. 1999. Delineation and identification of individual trees in eastern deciduous forest. In *Proceedings of the International Forum on Automated Interpretation of High Spatial Resolution Digital Imagery for Forestry*, 10–12 February 1998, Victoria, B.C. Pacific Forestry Center, Canadian Forest Service, Natural Resources Canada, Victoria, B.C. pp. 81–91.

Wulder, M., Niemann, K., and Goodenough, D. 2000. Local maximum filtering for the extraction of tree location and basal area from high resolution imagery. *Remote Sensing of Environment*, Vol. 73, pp. 103–114.